Oncogene (2010) 29, 105–116

www.nature.com/onc

ORIGINAL ARTICLE

Histone deacetylase inhibitors induce thyroid cancer-specific apoptosis through proteasome-dependent inhibition of TRAIL degradation

E Borbone[1,2,3], MT Berlingieri[1], F De Bellis[4], A Nebbioso[4], G Chiappetta[5], A Mai[6], L Altucci[4] and A Fusco[1,2,3]

[1]Istituto di Endocrinologia ed Oncologia Sperimentale, Naples, Italy; [2]NOGEC (Naples Oncogenomic Center)-CEINGE, Biotecnologie Avanzate, Napoli, Italy; [3]SEMM—European School of Molecular Medicine, Naples Site, Italy; [4]Dipartimento di Patologia Generale, Seconda Università degli Studi di Napoli, Naples, Italy; [5]Functional Genomic Unit, Experimental Oncology Department National Cancer Institute 'G. Pascale', Naples, Italy and [6]Istituto Pasteur, Fondazione Cenci-Bolognetti, Dipartimento di Chimica e Tecnologie del Farmaco, 'La Sapienza' Università di Roma, Rome, Italy

Anaplastic thyroid carcinoma (ATC) is considered one of the most aggressive malignancies, having a poor prognosis and being refractory to conventional chemotherapy and radiotherapy. Alteration in histone deacetylase (HDAC) activity has been reported in cancer, thus encouraging the development of HDAC inhibitors, whose antitumor action has been shown in both solid and hematological malignancies. However, the molecular basis for their tumor selectivity is unknown. To find an innovative therapy for the treatment of ATCs, we studied the effects of deacetylase inhibitors on thyroid tumorigenesis models. We show that HDACs 1 and 2 are overexpressed in ATCs compared with normal cells or benign tumors and that HDAC inhibitors induce apoptosis selectively in the fully transformed thyroid cells. Our results indicate that these phenomena are mediated by a novel action of HDAC inhibitors that reduces tumor necrosis factor-related apoptosis-inducing ligand protein degradation by affecting the ubiquitin-dependent pathway. Indeed, the combined treatment with HDAC and proteasome inhibitors results in synergistic apoptosis. These results strongly encourage the preclinical application of the combination deacetylase-proteasome inhibitors for the treatment of ATC.
Oncogene (2010) **29,** 105–116; doi:10.1038/onc.2009.306; published online 5 October 2009

Keywords: HDAC inhibitors; thyroid; carcinomas; apoptosis; TRAIL; proteasome

Introduction

Thyroid carcinoma of follicular cell origin is the most common endocrine malignancy, with an estimated 25 000 new cases diagnosed annually in the United States. The prognosis of thyroid carcinoma varies from the indolent well-differentiated papillary and follicular thyroid carcinomas, with a 30-year mortality rate of approximately 6%, to poorly differentiated thyroid carcinoma, which has a 60% 5-year survival rate, to anaplastic thyroid carcinoma (ATC), which is very aggressive and always fatal in a few months (Saltman *et al*., 2006). Surgical resection and radioactive iodine can be an effective treatment only for well-differentiated tumors. Conversely, ATC is refractory to conventional treatment as chemo- and radiotherapy, therefore representing an excellent target for innovative therapies.

In eukaryotes, genomic DNA is wrapped around histone octamers and the amino-terminal lysine residues of histone tails can be modified by acetylation, methylation and ubiquitination (Jenuwein and Allis, 2001). The balance between the acetylated and deacetylated states of chromatin is regulated by the histone acetyltransferase (HAT) and histone deacetylase (HDAC) enzymes (Marks *et al*., 2001; Kelly and Marks, 2005; Minucci and Pelicci, 2006). In fact, histone acetylation results in an opening of the chromatin fiber, whereas histone deacetylation causes a condensation of chromatin, preventing transcription factor accessibility and function. Mammalian HDACs are divided into four classes: (a) class I includes HDACs 1, 2, 3 and 8; (b) class II includes HDACs 4, 5, 6, 7, 9 and 10; (c) class III HDACs are the sirtuins (SIRT1-7); and (d) class IV contains HDAC 11 (Gallinari *et al*, 2007; Mai and Altucci, 2009; Altucci and Stunnenberg, 2009).

Aberrant regulation of gene expression attributed to alterations in histone acetyltransferase or HDAC recruitment and activity has constantly been found in both solid and hematologic tumors (Marks *et al*., 2001; Minucci and Pelicci, 2006; Mai and Altucci, 2009). Therefore, HDACs can be considered potential therapeutic targets for the treatment of human malignancies. There are at least five distinct classes of HDAC inhibitors (HDACis): short-chain fatty acids such as butyric acid, hydroxamic acids such as SAHA (suberoylanilide hydroxamic acid), electrophilic ketones, benzamides such as MS-275 (Hess-Stumpp *et al*., 2007) and cyclic peptides such as depsipeptide FK-228. HDACis induce growth arrest, differentiation and

Correspondence: Professor A Fusco, Dipartimento di Biologia e Patologia Cellulare e Molecolare, IEOS and University 'Federico II', via S Pansini 5, Naples 80131, Italy.
E-mail: alfusco@unina.it and
Professor L Altucci, Dipartimento di Patologia Generale, S.U.N., Vico L. De Crecchio 7, Naples 80138, Italy.
E-mail: lucia.altucci@unina2.it
Received 6 May 2009; revised 6 August 2009; accepted 23 August 2009; published online 5 October 2009

apoptosis of cancer cells *in vitro* and *in vivo* tumor-bearing animal models (Gallinari *et al*., 2007; Xu *et al*., 2007). HDACis have antitumor activity against different cancers at doses that are well tolerated by patients, and SAHA (Vorinostat, Zolinza) was approved quite recently by the US FDA for the treatment of cutaneous manifestations in patients with advanced, refractory cutaneous T-cell lymphoma (Duvic and Vu, 2007; Mann *et al*., 2007). The aim of our work has been to evaluate the possibility of an innovative therapy for ATC based on HDACis, investigating the effects and mechanisms of action of some HDACis on a model of rat thyroid cells transformed by the *v-ras*-Ki oncogene, which is one of the most common genetic lesions found in human tumors. We have chosen SAHA and MS-275, two HDACis in clinical trial, for the treatment of different types of tumors (Kelly *et al*., 2005; Kummar *et al*., 2007; Blumenschein *et al*., 2008; Garcia-Manero *et al*., 2008; Gore *et al*., 2008). SAHA inhibits both class I and II HDACs, whereas MS-275 is more selective inhibiting mostly HDACs 1 and 2. This difference is of great importance in understanding the role of HDAC enzymes and their inhibitions in thyroid cancer.

We first show that HDACs 1 and 2 are overexpressed in the anaplastic thyroid cancer tissues compared with normal thyroid tissues, and in the human and rat thyroid cancer cells with respect to the normal ones. Subsequently, we show that both HDACis induce apoptosis selectively in the FRTL-5 *v-ras*-Ki rat thyroid transformed cells, but not in the normal thyroid FRTL-5 Cl2 cells. The stabilization of the tumor necrosis factor-related apoptosis-inducing ligand (TRAIL) protein with its consequent accumulation in the cancer cells (i) accounts for the apoptotic effect of the HDACis, (ii) represents a novel mechanism for TRAIL-mediated apoptosis and (iii) is linked to the inhibition of HDACs 1 and 2.

Results

HDAC expression in human thyroid tumor biopsies and in rat thyroid cell lines

First, we evaluated the HDACs 1, 2 and 3 protein levels in normal thyroid, and in papillary, follicular and anaplastic thyroid carcinomas by immunohistochemistry. HDAC 1 and 2 proteins were found highly overexpressed in ATC samples compared with normal thyroid tissue (Figure 1a). The immunohistochemical results are summarized in Figure 1b. An intense nuclear staining for HDAC1 (Figure 1a, sub-panel 2) and HDAC2 (Figure 1a, sub-panel 4) was observed in the ATCs, whereas only a slight increase and weak nuclear staining was observed in papillary thyroid carcinomas and follicular thyroid carcinomas (data not shown) with respect to normal thyroid (Figure 1a, sub-panels 1 and 3). Conversely, HDAC1 and HDAC2 staining was comparable in thyroid adenomas, goiters and normal tissues (data not shown). HDAC3 staining did not show significant differences in ATCs compared with normal thyroid tissue (data not shown). Thus, the increase in HDACs 1 and 2 expression correlates positively with malignancy.

Subsequently, we analysed class I HDAC expression in rat thyroid cell lines transformed with different oncogenes and in human ATC cell lines with respect to the normal counterpart. The characteristics of the rat cell lines used are summarized in Table 1. HDAC1 protein levels were higher in tumorigenic cells (FRTL-5 *v-ras*-Ki and PC E1A + *v-raf*) and lower in nontumorigenic cells (PC *v-ras*-Ki) than in normal ones (FRTL-5 Cl2 and PC Cl3) (Figure 1c). HDAC2 protein was more abundant in FRTL-5 *v-ras*-Ki than in FRTL-5 Cl2. No significant differences in HDAC3 expression levels between normal and transformed cells were observed (Figure 1c). Analogous results were obtained in human ATC cell lines (FRO, FB1, 8505C, ACT-1) compared with normal primary thyroid cultures (Figure 1c). The expression of the specific HDACs 1 and 2 mRNA in rat thyroid cell lines, analysed by RNase protection assay, essentially supported the data on protein levels indicating that the expression of class I HDACs is regulated at the transcriptional level and that HDACs 1 and 2 are overexpressed in malignant thyroid cells (Figure 1d).

The HDACis, SAHA and MS-275, induce growth arrest and apoptosis in v-ras-Ki transformed rat thyroid cells

To test whether the overexpression of HDACs 1 and 2 corresponds to the increased effect of HDACis in tumor thyroid cells, we treated normal (FRTL-5 Cl2 and PC Cl3) and transformed (FRTL-5 *v-ras*-Ki and PC *v-ras*-Ki) rat thyroid cell lines with 5 μM SAHA and 5 μM MS-275 for 24, 48 and 72 h. We have chosen these concentrations as they have shown the optimal ones for inducing the accumulation of histone acetylation in cell cultures (Mitsiades *et al*., 2005). Fluorescence-activated cell sorting (FACS) analysis in Figure 2 shows that both SAHA and MS-275 induced apoptosis preferentially in the transformed cell lines, therefore confirming the HDAC expression data. The apoptotic effect was more evident in the highly tumorigenic cell line FRTL-5 *v-ras*-Ki (Figure 2b) than in PC *v-ras*-Ki, which did not show a malignant phenotype (Figure 2c), thus suggesting that HDACis might be more efficient in highly malignant thyroid tumors. Normal cell lines FRTL-5 Cl2 and PC Cl3 (Figure 2a) did not show any apoptotic effect after treatment. In full agreement with these findings, caspase-3 as effector caspase, casp-8, -9 initiator activities, in the HDACi-treated cells were activated in FRTL-5 *v-ras*-Ki but not in FRTL-5 Cl2 (Figure 2d), thus indicating that caspase-dependent apoptosis mediates cell death in transformed cells but not in normal thyroid cells. Caspase activation is also detectable after brief time of exposure to HDACis (Supplementary Figure 1).

In a similar experimental setting, the cell cycle analysis did not show significant differences between normal and tumor cell lines (Figures 3a and b). In fact, both cell lines undergo cell cycle arrest in the G1 phase after SAHA and MS-275 treatment, and the percentage of arrested cells increases with the time of exposure to

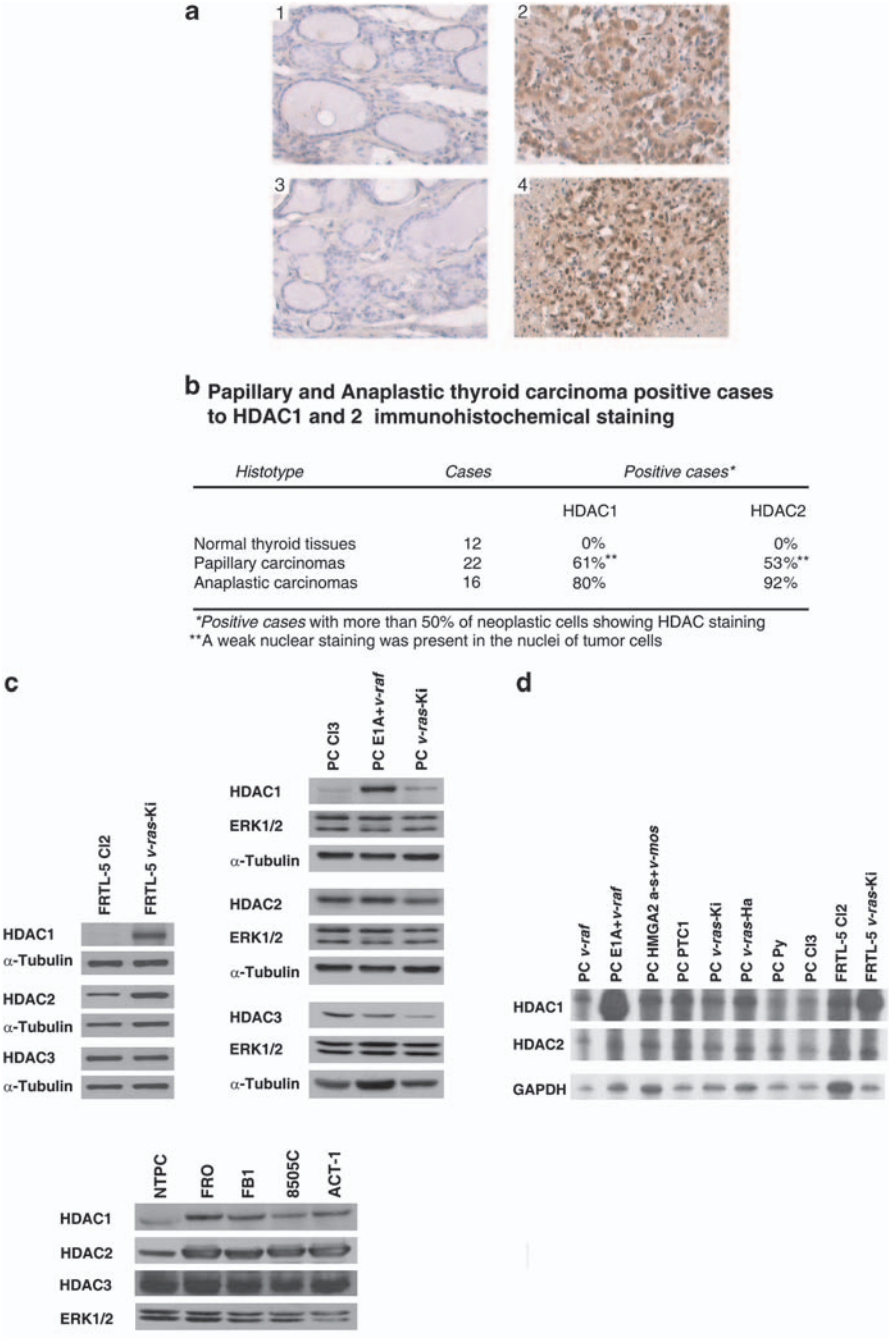

Figure 1 Analysis of histone deacetylases (HDACs) 1 and 2 expression in thyroid tumors and in rat thyroid cell lines. (**a**) Immunohistochemical analysis for HDAC1 (1–2) and HDAC2 (3–4) in normal and anaplastic thyroid tumors. Immunostaining of a normal thyroid (magnification $\times 200$). No immunoreactivity was observed (1 and 3). Immunostaining of anaplastic thyroid carcinomas (magnification $\times 200$). Strong nuclear staining was observed in (2 and 4) for HDAC 1 and 2, respectively. (**b**) Summary of the immunohistochemical data for HDAC 1 and 2 proteins. (**c**) Analysis of HDAC protein levels by western blot in normal and transformed rats and human thyroid cells. Blot against α-tubulin and ERK1/2 has been performed as control for equal protein loading. (**d**) HDAC mRNA expression analysis by multiple RNase protection assay in rat thyroid cells transformed with different oncogenes. GAPDH mRNA has been used as control for equal mRNA loading.

both drugs (Figures 3a and b). Moreover, neither SAHA nor MS-275 vehicles (dimethylsulfoxide and ethanol, respectively) affected cell cycle or apoptosis of the analysed cell lines at the concentration used (Figures 2 and 3). Furthermore, the evaluation of histone H3 acetylation by western blot analysis (Figure 3c) did not display significant differences of acetylated histone regulation among FRTL-5 Cl2 and their tumoral *ras* version. Indeed, we could detect an increase of H3 acetylation and a cell cycle arrest in both normal and cancer cells.

Interestingly, the compound MC1568, which is known to inhibit only class II HDACs (Mai *et al*., 2005; Inoue *et al*., 2006; Duong *et al*., 2008) (SAHA and

Table 1 Normal and transformed rat thyroid cell lines

Group	*Cell type*	*Oncogene*	*Differentiation status*
Nontumorigenic cell lines[a]	PC Cl3		Differentiated
	PC *v-ras*-Ki	*v-ras*-Ki	Undifferentiated
	PC *v-ras*-Ha	*v-ras*-Ha	Undifferentiated
	PC *v-raf*	*v-raf*	Undifferentiated
	PC HMGA2 a-s + *v-mos*	HMGA2 a-s + *v-mos*	Undifferentiated
	PC PTC-1	RET/PTC1	Undifferentiated
	FRTL-5 Cl2		Differentiated
Lowly tumorigenic cell lines[b]	PC Py MLV	Polyomavirus middle T	Differentiated
Highly tumorigenic cell lines[c]	PC E1A + *v-raf*	E1A + *v-raf*	Undifferentiated
	FRTL-5 *v-ras*-Ki	*v-ras*-Ki	Undifferentiated

[a]No tumors appeared after injection of 2×10^6 cells into six athymic mice.
[b]Tumors appeared at least 3 weeks after injection of 2×10^6 cells into athymic mice.
[c]Tumors appeared not later than 10 days after injection of 2×10^6 cells into athymic mice.

MS-275 inhibit class I–II and class I HDACs, respectively), induced only a slight G1 arrest, but did not cause apoptosis in both FRTL-5 Cl2 and FRTL-5 *v-ras*-Ki (Supplementary Figure 2). This evidence suggests that the apoptotic effects induced by SAHA and MS-275 in the FRTL-5 *v-ras*-Ki cells are attributed to the inhibition of class I HDACs and, in particular, to the block of HDACs 1 and 2, the only HDACs mainly inhibited by MS-275 (Nebbioso *et al*., 2005) and found overexpressed in thyroid carcinomas (Figure 1). To show that the apoptotic effects of HDACis are attributed to the inhibition of HDAC1 and HDAC2 activity, we transiently knocked down HDACs 1 and 2 by RNA interference in the FRTL-5 *v-ras*-Ki cell line and evaluated the apoptotic effect of SAHA. As shown in Supplementary Figure 3, single knockdown of either HDAC1 or HDAC2 caused a reduction of about 50% in the number of SAHA-induced apoptotic cells, whereas double knockdown caused a reduction of about 70% in the number of SAHA-induced apoptotic cells. Therefore, these results indicate that the apoptotic effect of SAHA is attributed to the inhibition of HDAC1 and HDAC2 activity. Finally, to evaluate the extent of SAHA and MS-275 effects in these thyroid cell lines, we treated FRTL-5 Cl2 and FRTL-5 *v-ras*-Ki cell lines for 24, 48 and 72 h, removing the drugs and allowing the cells to grow for an additional 24 and 48 h. As shown in Figure 3d, FRTL-5 Cl2 re-entered the S phase after drug removal, whereas FRTL-5 *v-ras*-Ki treated for 72 h, but not those treated for 24 and 48 h (data not shown), remained blocked in the G1 phase going toward death. These results corroborate the low toxicity of SAHA and MS-275 for normal thyroid cells, thus stressing the selectively induced cell death caused by HDACis in transformed cells.

SAHA and MS-275 induce TRAIL in transformed FRTL-5 v-ras-Ki thyroid cells

To understand the molecular events occurring upon HDACi treatment and underlying selective tumor cell death, we evaluated the levels of known proteins involved in apoptosis such as Bax, Bcl2 and BclxL in both FRTL-5 Cl2 and FRTL-5 *v-ras*-Ki before and after treatment. The treatment with both HDACis did not affect the protein levels of Bax and Bcl2, whereas BclxL was upregulated in normal cells and downregulated in cancer cells (Supplementary Figure 4). High levels of BclxL could be important in blocking the apoptotic process in normal cells. When cell cycle-related proteins were investigated, p21/WAF1 was induced only by MS-275 in both normal and transformed cells after 16 h of treatment, whereas p27/Kip1 was induced by both drugs only in normal cells. Therefore, it is reasonable to speculate that p27 induction might be responsible for the cell cycle arrest caused by these HDACis in normal thyroid cells.

Tumor necrosis factor-related apoptosis-inducing ligand (TNFSF10, tumor necrosis factor ligand superfamily member 10) is a member of the tumor necrosis factor cytokine family that induces apoptosis on binding to its death receptors TRAIL receptor 1 (death receptor 4, DR4) and TRAIL receptor 2 (death receptor 5, DR5) (Johnstone *et al*., 2008). The tumor-selective action of HDACis has been shown to be mediated mainly by the proapoptotic ligand TRAIL, which is induced at the transcriptional level only in transformed cells (Nebbioso *et al*., 2005; Earel *et al*., 2006; Hall and Cleveland, 2007; Johnstone *et al*., 2008; Macher-Goeppinger *et al*., 2009). TRAIL preferentially kills transformed but not normal cells, both *in vitro* and *in vivo*, and the mechanisms for this selectivity are presently obscure (Ashkenazi, 2002; Mahalingam *et al*., 2009).

Therefore, we analysed TRAIL expression by western blot in normal and transformed cells. As shown in Figure 4a (top), both SAHA and MS-275 induced TRAIL protein only in FRTL-5 *v-ras*-Ki cells. We also confirmed this result evaluating surface TRAIL protein levels by FACS (Figure 4a, bottom). Then, we assessed surface versus intracellular TRAIL expression by flow cytometry. SAHA causes a similar induction of TRAIL expression in intact cells compared with permeabilized cells, suggesting that all SAHA-induced TRAIL proteins are on the cell membrane (Supplementary Figure 5a,b and c). At odds with previously reported data (Insinga *et al*., 2005; Nebbioso *et al*., 2005), semiquantitative (Figure 4b, top) and quantitative (Figure 4b, bottom) reverse transcription (RT)–PCR analyses do not show significant differences between treated and untreated, normal and transformed cells in TRAIL

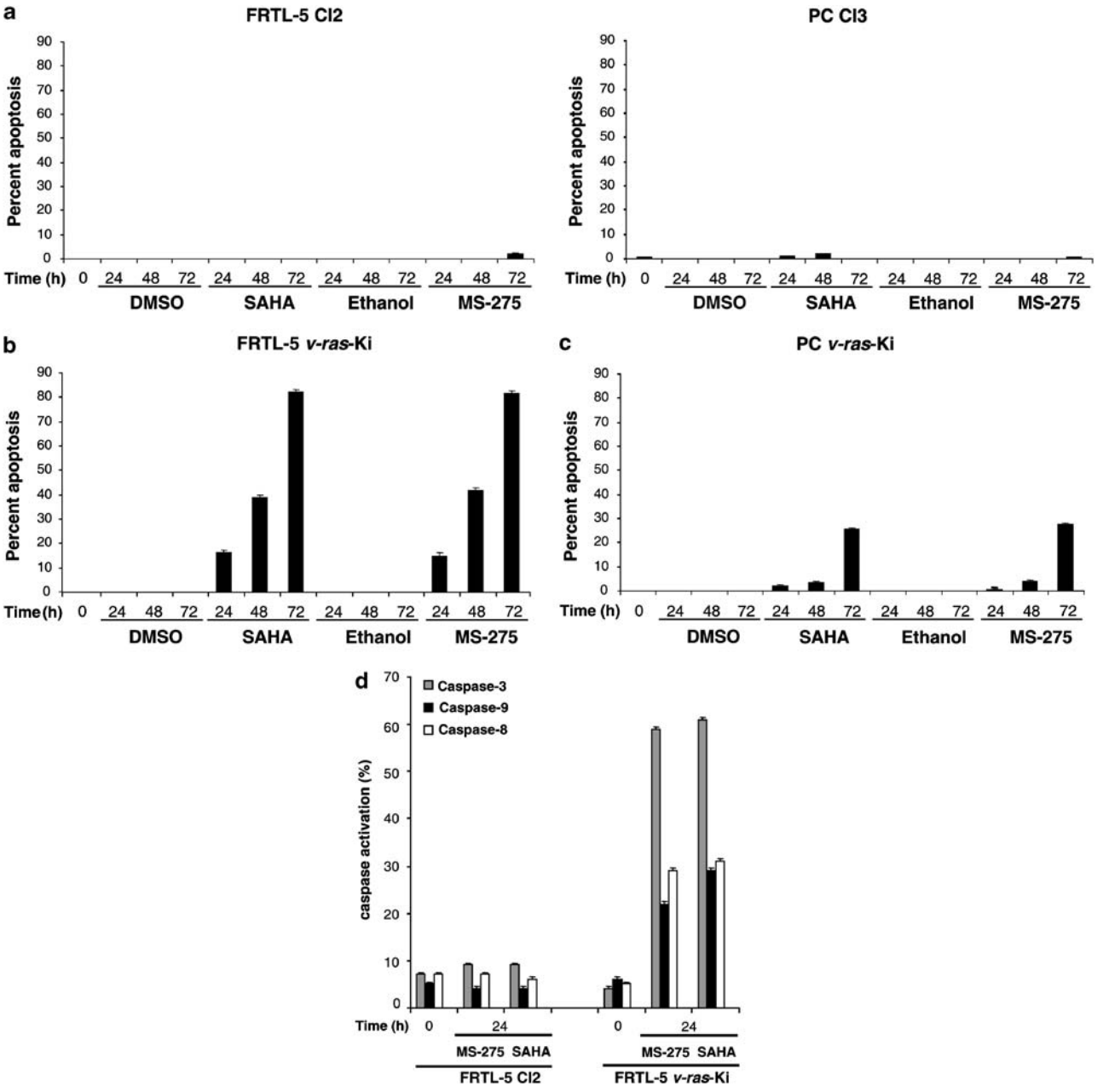

Figure 2 SAHA and MS-275 induce apoptosis in transformed thyroid cells. Fluorescence-activated cell sorting (FACS) analysis of normal (**a**) and transformed (**b** and **c**) rat thyroid cells, treated with SAHA and MS-275 for 24, 48 and 72 h, to evaluate the apoptotic effect. Apoptosis is expressed as the percentage of dead cells in the cell population analysed. The apoptotic cells annexin-V+/ propidium iodide– were considered. FACS analysis of FRTL-5 Cl2 and FRTL-5 *v-ras*-Ki treated for 24 h with SAHA and MS-275 to assess drug-induced activation of caspases-3, -8, -9 (**d**). The scale bars represent the mean ± s.e. ($n = 3$). Results are reported as mean expression values of three independent experiments, with error bars indicating s.e.

mRNA expression level, thus suggesting that TRAIL regulation by HDACis occurs at the post-transcriptional level. We also confirmed the specificity of this mechanism for thyroid carcinoma cells evaluating TRAIL expression in human acute myeloid leukemia cell lines (K562 and NB4) as positive control by quantitative RT–PCR. As shown in Supplementary Figure 6, HDACis induce an evident increase in the TRAIL mRNA level with respect to untreated cells.

TRAIL is the main mediator of cell death induced by SAHA

Intrigued by the TRAIL induction stimulated by HDACis in tumor thyroid cells, we transiently knocked down TRAIL by an interference methodology in the FRTL-5 Cl2 and FRTL-5 *v-ras*-Ki cell lines. The TRAIL mRNA expression was drastically reduced in the TRAIL siRNA-transfected cells as the efficiency of TRAIL knockdown, evaluated by quantitative

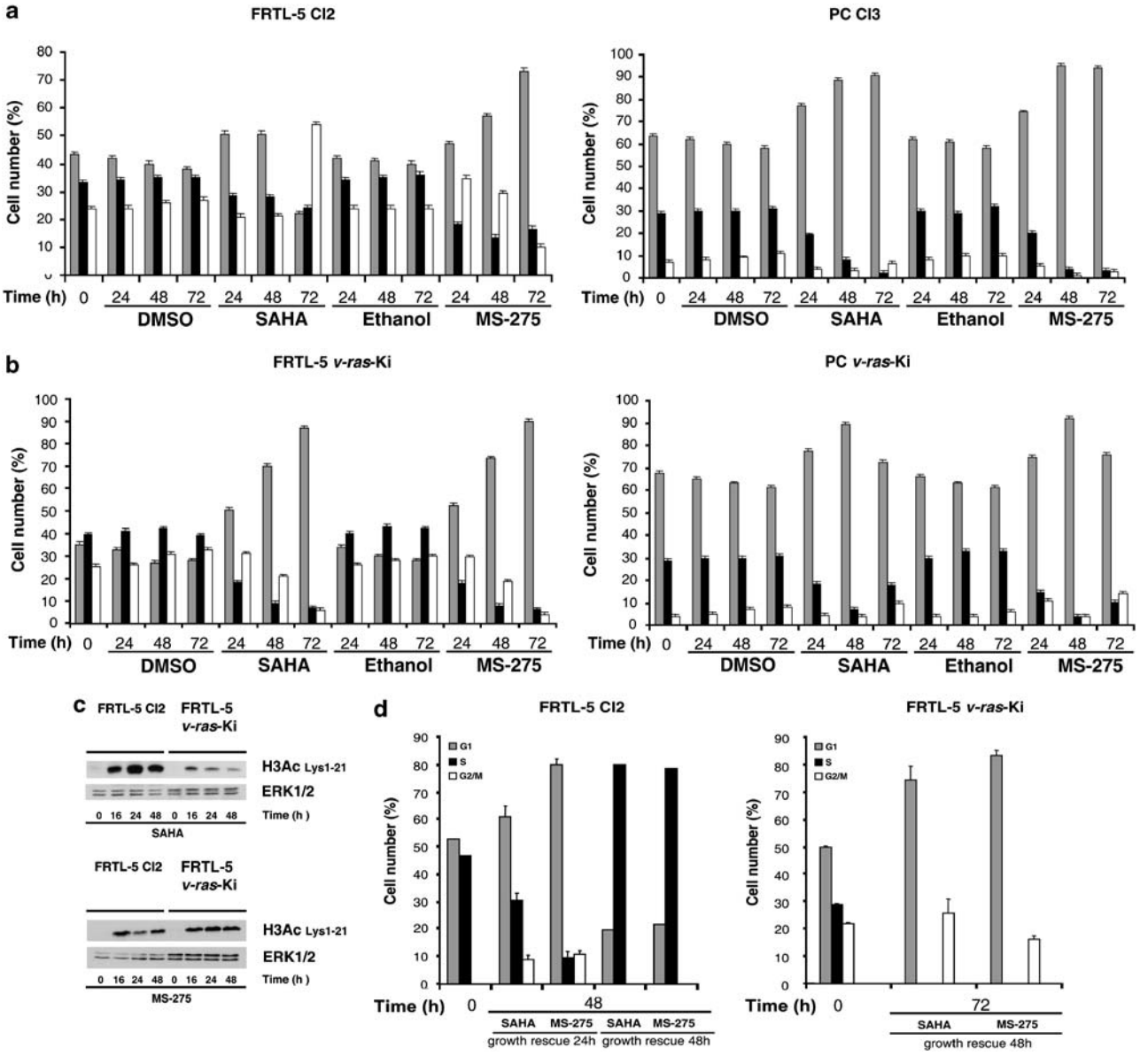

Figure 3 SAHA and MS-275 induce growth arrest in rat thyroid cells. (**a** and **b**) Fluorescence-activated cell sorting (FACS) analysis of normal and transformed rat thyroid cells, treated for 24, 48 and 72 h with SAHA and MS-275, to analyse the cell cycle. G1 phase (grey bars), S phase (black bars) and G2/M phase (white bars). (**c**) Western blot analysis of acetylated histone H3 in both FRTL-5 Cl2 and FRTL-5 *v-ras*-Ki treated with SAHA and MS-275. ERK1/2 has been performed as control for equal protein loading. (**d**) Cell cycle analysis, performed by FACS, of FRTL-5 Cl2 and FRTL-5 *v-ras*-Ki treated with SAHA and MS-275 for 48 and 72 h, respectively, and grown after removal of both drugs. The scale bars represent the mean ± s.e ($n = 3$). Results are reported as mean expression values of three independent experiments, with error bars indicating s.e.

Figure 4 Expression analysis of death ligand tumor necrosis factor-related apoptosis-inducing ligand (TRAIL) in normal and transformed rat thyroid cell lines (**a** and **b**). Western blot (**a**, top) and flow cytometry analysis (**a**, bottom) of TRAIL protein expression in FRTL-5 Cl2 and FRTL-5 *v-ras*-Ki cells treated with SAHA and MS-275. Blot against ERK1/2 has been performed as control for equal protein loading**.** Semiquantitative (**b**, top) and quantitative (**b**, bottom) reverse transcription (RT)–PCR analyses of TRAIL expression at mRNA level. β-Actin gene expression was evaluated as control to normalize the amount of used RNAs. The fold change indicates the relative change in expression levels between treated and untreated samples, assuming that the value of the untreated sample is equal to 0. G6PDH gene expression was evaluated as control for normalization. TRAIL RNA interference in FRTL-5 Cl2 and FRTL-5 *v-ras*-Ki treated with SAHA (**c** and **d**). Quantitative RT–PCR analysis of TRAIL mRNA level in FRTL-5 Cl2 and FRTL-5 *v-ras*-Ki cells transfected with scramble or TRAIL small interfering RNAs (siRNAs) and treated with SAHA for 24 h (**c**, bottom). The fold change indicates the relative change in expression levels between scramble siRNA-transfected cells and TRAIL siRNA-transfected cells, assuming that the value of the untreated sample is equal to 0. G6PDH gene expression was evaluated as control for normalization of the used RNAs. Fluorescence-activated cell sorting (FACS) analysis to quantify the TRAIL protein cell-surface level in FRTL-5 Cl2 and FRTL-5 *v-ras*-Ki cells transfected with scramble or TRAIL siRNAs and treated with SAHA for 24 h (**c**, top). FACS analysis for quantification of apoptotic cells (**d**, bottom) and caspase-3 activation (**d**, top) in FRTL-5 Cl2 and FRTL-5 *v-ras*-Ki cells transfected with scramble or TRAIL siRNAs and treated with SAHA for 24 h (**d**). The scale bars represent the mean ± s.e. ($n = 3$). Results are reported as mean expression values of three independent experiments, with error bars indicating s.e.

RT–PCR (Figure 4c, bottom) and TRAIL protein cell-surface level analysis (Figure 4c, top), clearly shows. Interestingly, TRAIL silencing caused a significant reduction in both the level of apoptotic FRTL-5 *v-ras*-Ki cells (Figure 4d, bottom) and their caspase-3 activation (Figure 4d, top) compared with the same

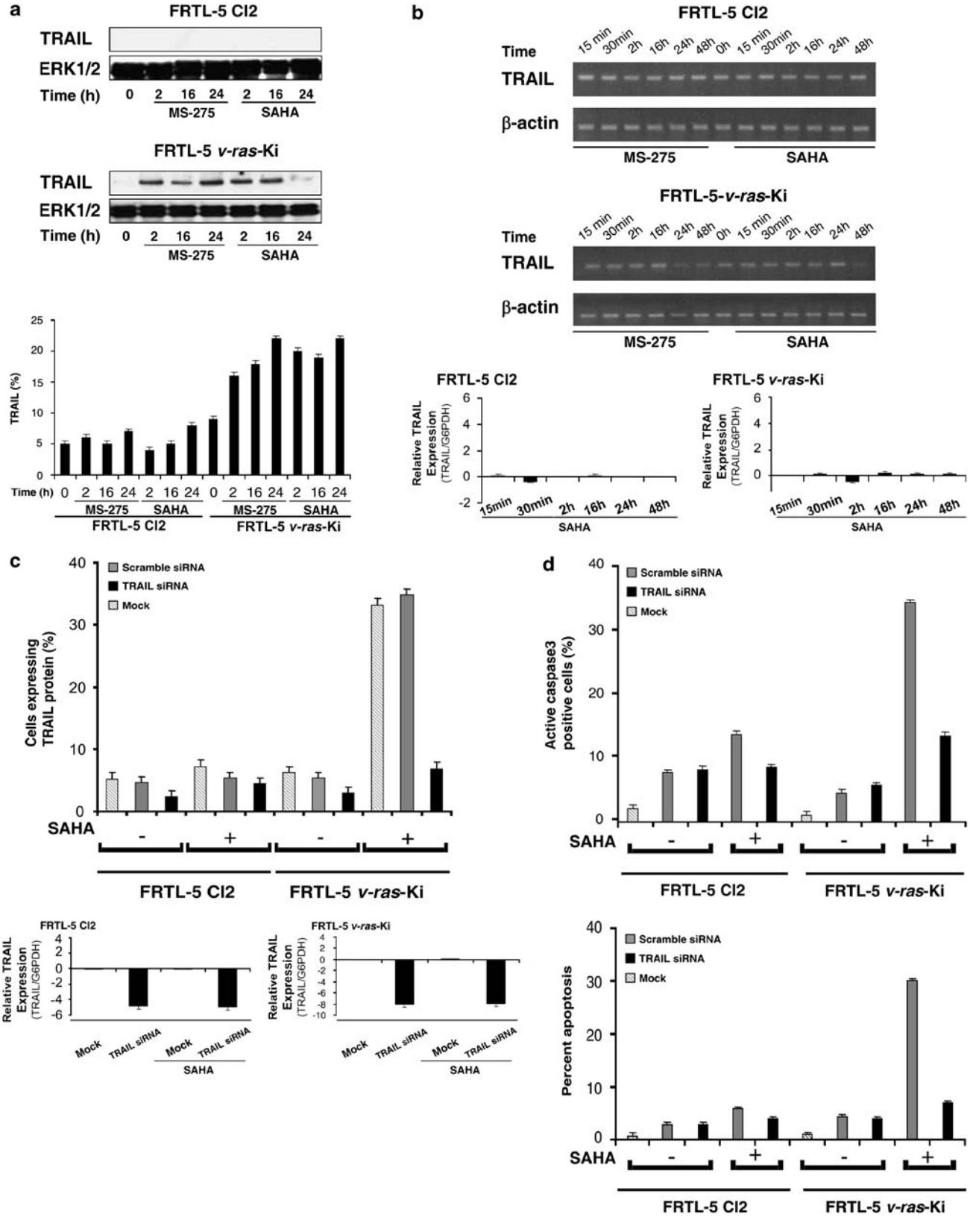

SAHA-treated cells transfected with a scramble small interfering RNA. The analysis of caspase-3 performed only in the transfected cells ensured that the decrease in apoptosis occurred for TRAIL silencing. This result indicates that TRAIL is a main mediator of the apoptosis induced by HDACis in transformed thyroid cells. Moreover, to show that TRAIL expression does not affect apoptosis automatically, we examined the DR5 receptor protein expression by western blot in both FRTL-5 Cl2 and FRTL-5 *v-ras*-Ki treated with SAHA and MS-275 for 2, 16 and 24 h. As shown in Supplementary Figure 7, HDACis do not modify DR5 protein levels, thus indicating that HDACi-induced apoptosis in transformed cells is related to TRAIL ligand itself rather than to its receptor levels.

SAHA and MS-275 induce TRAIL protein stabilization

As our data indicate that SAHA and MS-275 induce TRAIL only at the protein level, we hypothesized that HDACis stabilized TRAIL by altering its degradation, likely by proteasome mediation. In fact, the ubiquitin-proteasome pathway mediates the degradation of key proteins regulating the cell cycle, transcription, signal transduction and apoptosis having a central role in the regulation of these phenomena. To show this hypothesis, we treated both FRTL-5 Cl2 and FRTL-5 *v-ras*-Ki cells with 1 μM or 2.5 μM SAHA in the presence or absence of 1 μm MG132, a known proteasome inhibitor. The combined treatment of SAHA with MG132 resulted in a significant increase in TRAIL protein level in transformed cells in comparison with the single treatments (Figure 5a). Conversely, and in agreement with our previous data (Figure 4a), TRAIL was not detectable in both treated and untreated normal cells. The evaluation of the cell cycle and apoptosis by FACS in normal and transformed thyroid cells in these experimental settings showed a different effect on these cell lines. In fact, FRTL-5 Cl2 normal thyroid cells were arrested in the G1 phase but did not undergo apoptosis after treatment (Supplementary Figure 8a and Figure 5b), whereas FRTL-5 v-ras-Ki treated with both SAHA and MG132 showed an apoptosis much higher than that observed for the cells treated singularly (24% with SAHA, 10% with MG132). These results strongly indicate that SAHA and MG132 synergize in killing tumor cells through the stabilization of the death ligand TRAIL. Analogous results were obtained with the combination MS-275-MG132 (Supplementary Figure 8b and c). However, the HDACi effect on proteasome-dependent protein degradation seems to be specific for TRAIL protein. In fact, HDACis do not alter the level of expression of other proteasome-degraded proteins such as Bax and Bcl-2 (Supplementary Figure 4).

To confirm that TRAIL is stabilized by HDACis, we analysed the half-life of TRAIL in FRTL-5 *v-ras*-Ki treated with 5 μM SAHA for 24 h and 5 μg/ml cycloheximide for 2, 4 and 8 h to block mRNA translation. As shown in Figure 5c, TRAIL protein disappeared after 8 h in FRTL-5 *v-ras*-Ki treated only with cycloheximide, whereas it was still present after 8 h in cycloheximide-SAHA-treated cells, indicating that SAHA treatment induces an increase of the TRAIL protein half-life.

To further show that SAHA reduces TRAIL protein degradation affecting the ubiquitin-dependent pathway,

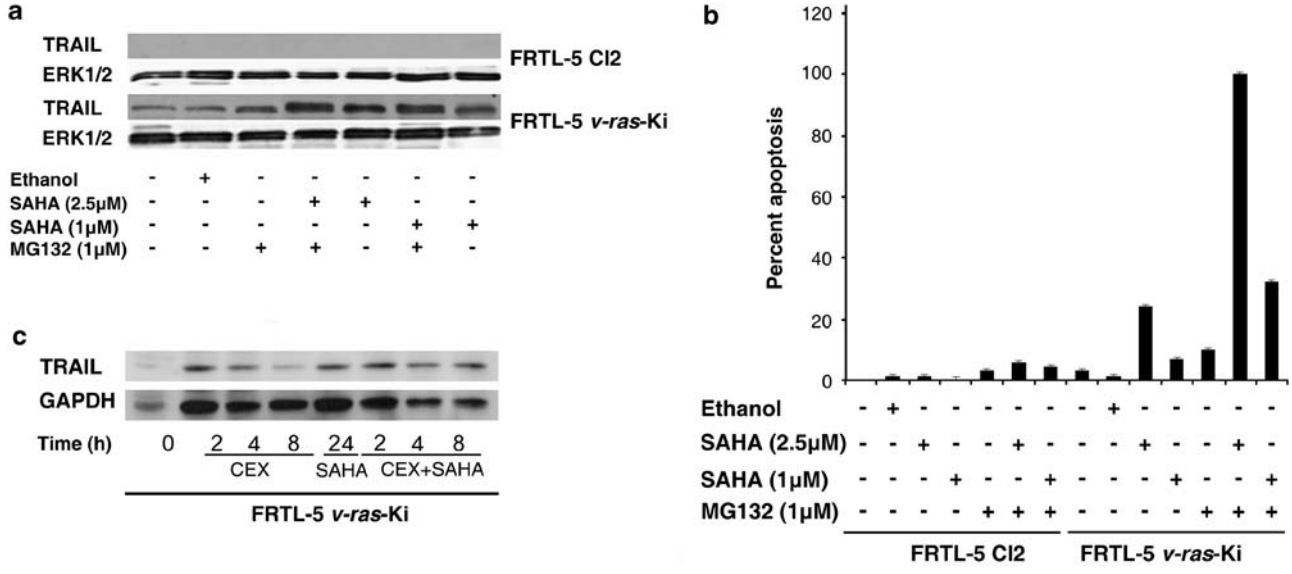

Figure 5 SAHA and MG132 synergize in induction of apoptosis through stabilization of the death ligand tumor necrosis factor-related apoptosis-inducing ligand (TRAIL). (**a**) Western blot for TRAIL of whole extracts of FRTL-5 Cl2 and FRTL-5 *v-ras*-Ki cells treated with SAHA, MG132 or the combination SAHA + MG132. Ethanol has been used as a vehicle for MG132. Blot against ERK1/2 has been performed as control for equal protein loading. (**b**) Fluorescence-activated cell sorting analysis to quantify apoptosis of FRTL-5 Cl2 and FRTL-5 *v-ras*-Ki cells treated with SAHA, MG132 or the SAHA + MG132 combination. The scale bars represent the mean ± s.e. ($n = 3$). Results are reported as mean expression values of three independent experiments, with error bars indicating s.e. (**c**) TRAIL immunoblot of whole extracts of FRTL-5 *v-ras*-Ki cells treated with 5 μM SAHA for 24 h and 5 μg/ml cycloheximide (CEX) for 2, 4 and 8 h. GAPDH has been performed as control for equal protein loading.

we co-transfected FRTL-5 *v-ras*-Ki cells with pEGFP-N1 and p-Ubi-His or with pEGFP-TRAIL and p-Ubi-His plasmids. We determined the degradation of the TRAIL-GFP fusion protein by evaluating cell fluorescence by FACS after treatment with 5 μM SAHA for 16 h. The amount of exogenous TRAIL, proportional to the cell fluorescence, increased after treatment with SAHA, whereas it was reduced after overexpression of ubiquitin (Figure 6a). Taken together, these results indicate that SAHA reduces TRAIL degradation in thyroid-transformed cells by altering the ubiquitin-dependent pathway of degradation. We performed an immunoprecipitation experiment to investigate whether TRAIL can be ubiquitinated. Then, we treated FRTL-5 *v-ras*-Ki with SAHA for 24 h and immunoprecipitated cell lysates with a mouse monoclonal anti-ubiquitin antibody. Subsequently, ubiquitinated TRAIL protein was detected by western blot analysis using an anti-TRAIL antibody. As shown in Figure 6b, we were able to detect a band of ~72 kDa that is attributed to TRAIL protein (33 kDa) bound to 4–5 ubiquitin molecules (~8 kDa). This result confirms that TRAIL protein is a target of the ubiquitin-proteasome pathway. In agreement with our finding that SAHA stabilizes TRAIL protein, the amount of ubiquitinated TRAIL is lower in SAHA-treated cells with respect to vehicle-treated cells (Figure 6b). However, it is possible that SAHA could reduce the TRAIL protein degradation also affecting the ubiquitin-proteasome pathway downstream of the ubiquitination event. Finally, to show that our findings can also be extended to human anaplastic cells and serve as an alternative therapy for thyroid anaplastic cancer, we verified the efficacy of the combination MG132 + SAHA on FRO, a human anaplastic thyroid cell line. We treated the FRO cells (Fagin *et al*., 1993) with 5 μM SAHA, 0.25 μM MG132 or with the combination of both drugs. Although the single treatments did not induce cell cycle arrest (Supplementary Figure 9a), the combination SAHA + MG132 had a synergistic effect in inducing apoptosis in FRO cells as previously shown for FRTL-5 *v-ras*-Ki cells (Figure 5c). Indeed, the combined treatment caused an evident increase in apoptosis compared with the single treatments (Supplementary Figure 9b). Analogous results were obtained for FB1 (Supplementary Figure 9c and d), another human anaplastic thyroid cell line (Fiore *et al*., 1997), thus suggesting that this combination treatment might be useful against anaplastic thyroid cancer.

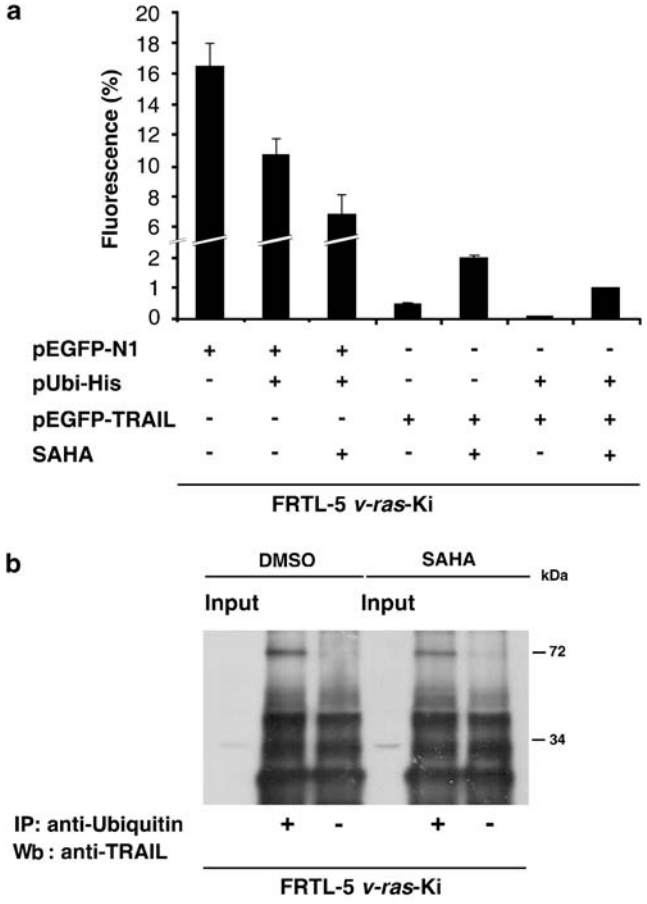

Figure 6 SAHA reduces tumor necrosis factor-related apoptosis-inducing ligand (TRAIL) degradation by affecting the ubiquitination pathway. (**a**) Fluorescence-activated cell sorting (FACS) analysis to quantify fluorescence and stability of TRAIL-GFP fusion protein in FRTL-5 *v-ras*-Ki cells transfected with pEGFP-TRAIL, in the presence or absence of p-Ubi-His, and treated with SAHA. The scale bars represent the mean ± s.e. ($n = 3$). Results are reported as mean expression values of three independent experiments, with error bars indicating s.e. (**b**) Western blot (Wb) analysis with anti-TRAIL antibody of lysates extracted from FRTL-5 *v-ras*-Ki treated with dimethylsulfoxide or SAHA and immunoprecipitated (IP) with anti-ubiquitin antibody. The upper band indicates the ubiquitinated form of TRAIL protein migrating at 72 kDa.

Discussion

In this study, we have analysed the effects of two potent HDACis, namely SAHA (Vorinostat, Zolinza) and MS-275, in a well-defined cell system where the process of tumor transformation is well known, allowing a better comprehension of the mechanisms through which these drugs may act. The cell system studied here is represented by the rat thyroid cells infected with the Kirsten murine sarcoma virus carrying the v-*ras*-Ki oncogene (Fusco *et al*., 1987). These cells have lost the expression of the typical markers of thyroid differentiation, grow with a high efficiency in soft agar and induce tumors after injection into athymic mice. The critical role of *ras* gene activation in some thyroid cancer histotypes was confirmed by the induction of thyroid follicular carcinomas associated with lung metastasis following the injection of the Kirsten murine sarcoma virus into the thyroid gland of adult Fischer rats (Portella *et al*., 1989). The important role of *ras* oncogene in thyroid cancer was also shown in human follicular and anaplastic carcinoma in which the frequency of mutation in this gene is about 50% (Nikiforova *et al*., 2003).

SAHA and MS-275 have a different spectrum of action, as SAHA inhibits both class I and II HDACs,

whereas MS-275 inhibits only HDACs 1, 2 and 3 to a lower extent. They are already objects of clinical trials for the treatment of solid and hematological tumors with minor side effects (Glaser, 2007; Mai and Altucci, 2009). SAHA (Vorinostat, Zolinza) in particular has been approved by the Food and Drug Administration for the treatment of cutaneous manifestations of T-cell lymphoma in cancer patients. Previous studies have shown that SAHA arrests cell growth, induces apoptosis of a wide variety of transformed cells and inhibits tumor growth in animal models bearing solid tumors and hematological malignancies (Marks, 2007). Indeed, SAHA and MS-275 display antitumor activity in acute myeloid leukemia mediated by both p21/WAF1 and the tumor-selective death ligand TRAIL (Altucci *et al*., 2005; Insinga *et al*., 2005; Nebbioso *et al*., 2005).

In this study, we show that both SAHA and MS-275 induce apoptosis in rat thyroid-transformed cells with highly malignant phenotype, but not in normal cells. The increase in the activities of caspases-8 and -9, induced by the treatment with these drugs, suggested that both SAHA and MS-275 could activate mitochondrial and death receptor apoptotic pathways. However, we obtained a decrease in HDACi-mediated apoptosis by the silencing TRAIL expression, thus indicating that TRAIL is a key mediator of HDACi-induced apoptosis in thyroid carcinoma cells. The absence of significant differences in TRAIL transcript levels in both normal and transformed cells suggested TRAIL regulation at the protein level. This hypothesis appears to be confirmed by (i) the synergistic apoptotic effect of SAHA and the proteasome inhibitor MG132; (ii) the proportional increase in TRAIL protein level in the combo treatment with respect to the single one; and (iii) the clear increase in TRAIL half-life induced by SAHA.

The ubiquitination of TRAIL, reported here for the first time, represents an important mechanism for the regulation of the TRAIL protein level and may suggest new approaches to a better induction of its stabilization. Therefore, our results suggest a new molecular mechanism by which HDACis regulate cell death through a ubiquitin-proteasome-dependent stabilization of TRAIL. Our demonstration that (i) TRAIL is degraded through a ubiquitin-proteasome pathway and (ii) SAHA stabilizes TRAIL protein by reducing its ubiquitination and proteasome degradation is a fully novel finding that explains, at the molecular level, why the combination of a proteasome inhibitor and an HDACi might be successful in the treatment of anaplastic thyroid cancers. The efficacy of HDACis on human thyroid carcinoma cell lines has already been reported (Mitsiades *et al*., 2005). However, on the basis of the proteasome-dependent TRAIL stabilization, our results unveil the mechanism by which the HDACi selectively kill cancer cells. Moreover, we show that the combination of HDACi with a proteasome inhibitor has a much higher efficacy, with respect to the treatment with HDACi alone, inducing the death of cell lines deriving from ATCs. In agreement with our findings, the synergism of proteasome inhibitors with HDACis has recently been reported in glioma, in cervical cancer and in leukemia (Miller *et al*., 2007, 2009; Dai *et al*., 2008; Yu *et al*., 2008; Lin *et al*., 2009), strongly supporting our molecular model and suggesting the application of this combined treatment in other types of cancers.

Therefore, the synergism between MG132 and SAHA, through TRAIL signaling pathway activation, encourages the preclinical application of the combination of HDACis with proteasome inhibitors such as Bortezomib, or with drugs activating the TRAIL apoptotic pathway. In conclusion, our findings may contribute to the development of a novel, molecularly based approach in thyroid cancer treatment.

Materials and methods

Cell lines

FRTL-5 Cl2, PC Cl3, FRTL-5 *v-ras*-Ki and PC *v-ras*-Ki are rat thyroid epithelial cell lines. Rat and human thyroid cell lines were described previously (Fusco *et al*., 1987; Fagin *et al*., 1993; Fiore *et al*., 1997; Pallante *et al*., 2005; Nappi *et al*., 2009).

Chemicals

MS-275 (a kind gift from Bayer-Schering, Berlin, Germany) and MG132 (Calbiochem, Nottingham, UK) were dissolved in ethanol, whereas SAHA (Alexis, Florence, Italy) and MC1568 were dissolved in dimethylsulfoxide.

Apoptosis and cell cycle

Normal and transformed rat thyroid cell lines were treated with 5 μM SAHA, 5 μM MS-275 and 5 μM MC1568 for 24, 48 and 72 h. Apoptosis was quantified by propidium iodide-Annexin-V double staining (Altucci *et al*., 2001). The apoptotic cells Annexin V-positive/propidium iodide-negative were considered. Recycling experiments: after treatment of the cells, the medium was replaced with fresh medium and the cells remained in culture for an additional 24 and 48 h. Samples were acquired on an FACS-Calibur flow cytometer using the Cell Quest software (Becton Dickinson, Milan, Italy) and analysed by standard procedures using the same software and the ModFit LT version 3 Software (Verity, Topsham, ME, USA) as previously reported (Nebbioso *et al*., 2005; Scognamiglio *et al*., 2008).

Caspase assay

FRTL-5 Cl2 and FRTL-5 *v-ras*-Ki were treated with 5 μM SAHA and 5 μM MS-275 for 8, 16 and 24 h. Caspases-3, -9 and -8 activities were measured by FACS following the manufacturer's instructions (B-Bridge, Mountain View, CA, USA) (Bontempo *et al*., 2007).

RNase protection assay and RT–PCR

The ribonuclease (RNase) Protection Assay was performed according to standard procedures (Pharmingen, San Diego, CA, USA) as previously reported (Altucci *et al*., 2001; Scognamiglio *et al*., 2008). Probes used for specific HDAC detection in rats are available on request. FRTL-5 Cl2 and FRTL-5 *v-ras*-Ki RNA have been used for RT–PCR according to the manufacturer's instructions (Qiagen, Milan, Italy). Quantitative RT–PCR was performed as previously described (Pallante *et al*., 2008). Primer sequences are available as Supplementary Materials and methods.

RNA interference

See Supplementary Materials and methods.

Antibodies and immunoanalyses
Protein extracts were prepared as previously described (Pallante *et al*., 2005). The antibodies used were as follows: acetylated-H3 (Ac-H3) (Upstate, Billerica, MA, USA); p27/Kip1 (BD Transduction Laboratories, San Jose, CA, USA); Bcl-2 (Stressgen, Ann Arbor, Michigan, USA); p21/Waf-1, Bax, HDAC2 and GAPDH (Santa Cruz Biotechnology, Santa Cruz, CA, USA); HDAC1, HDAC3, ERK1/2 and Ubiquitin (Cell Signaling, Danvers, MA, USA); BclxL (R&D Systems, Milan, Italy), TRAIL (Chemicon, Billerica, MA, USA); α-tubulin and DR5 (Sigma, Milan, Italy).

Immunohistochemistry
The immunohistochemical analysis for HDAC1, HDAC2 and HDAC3 was performed as previously described (Chiappetta *et al*., 2008). We declare that informed consent for the scientific use of biological material was obtained from all patients.

Protein stability
FRTL-5 Cl2 and FRTL-5 *v-ras*-Ki were treated with 5 μM SAHA for 24 h and with 5 μg/ml cycloheximide for 2, 4 and 8 h. After treatment, cells were harvested and protein extracts were analysed by western blot.

Immunoprecipitation
FRTL-5 *v-ras*-Ki cells were treated with dimethylsulfoxide or 5 μM SAHA for 24 h. Cell lysates were prepared as previously described (Iervolino *et al*., 2006) and incubated with anti-ubiquitin for 2 h at 4 °C. The immunocomplexes were precipitated with protein A/G-Agarose (Santa Cruz Biotechnology) overnight at 4 °C. Western blot analysis was performed with an anti-TRAIL antibody.

Drug combination studies
FRTL-5 Cl2 and FRTL-5 *v-ras*-Ki were treated with 1 μM MG132 for 3 h and then with 1 μM or 2.5 μM SAHA or 5 μM MS-275 for 24 h. FRO and FB1 cells were treated with 0.25 μM or 2 μM MG132, respectively, for 3 h and then with 5 μM SAHA for 24 h. Cells were collected and analysed by FACS.

Degradation assay
FRTL-5 *v-ras*-Ki cells were co-transfected with GFP (pEGFP-N1) (Clontech, Mountain View, CA, USA) and histidine-tagged ubiquitin (p-Ubi-His) plasmids or with TRAIL-GFP fusion protein (pEGFP-TRAIL) (Addgene, Cambridge, MA, USA) and histidine-tagged ubiquitin (p-Ubi-His) plasmids. Cells were treated with SAHA and analysed by FACS.

Conflict of interest

The authors declare no conflict of interest.

Acknowledgements

This work was supported by grants from the Associazione Italiana Ricerca sul Cancro (AIRC), and from the Ministero dell'Università e della Ricerca Scientifica e Tecnologica (MIUR); EU (LSHC-CT2005-518417; HEALTH-F2-2007-200620; HEALTH-F4-2007-200767; HEALTH-F4-2009-221952) and the NOGEC-Naples Oncogenomic Center. We thank Konstantina Vergadou for revising and editing the article, Mario Berardone for the artwork, and Pollice A for providing some plasmids.

References

Altucci L, Clarke N, Nebbioso A, Scognamiglio A, Gronemeyer H. (2005). Acute myeloid leukemia: therapeutic impact of epigenetic drugs. *Int J Biochem Cell Biol* **37**: 1752–1762.

Altucci L, Rossin A, Raffelsberger W, Reitmair A, Chomienne C, Gronemeyer H. (2001). Retinoic acid-induced apoptosis in leukemia cells is mediated by paracrine action of tumor-selective death ligand TRAIL. *Nat Med* **7**: 680–686.

Altucci L, Stunnenberg HG. (2009). Time for epigenetics. *Int J Biochem Cell Biol* **41**: 2–3.

Ashkenazi A. (2002). Targeting death and decoy receptors of the tumour-necrosis factor superfamily. *Nat Rev Cancer* **2**: 420–430.

Blumenschein Jr GR., Kies MS, Papadimitrakopoulou VA, Lu C, Kumar AJ, Ricker JL *et al* (2008). Phase II trial of the histone deacetylase inhibitor vorinostat (Zolinza, suberoylanilide hydroxamic acid, SAHA) in patients with recurrent and/or metastatic head and neck cancer. *Invest New Drugs* **26**: 81–87.

Bontempo P, Mita L, Miceli M, Doto A, Nebbioso A, De Bellis F *et al* (2007). Feijoa sellowiana derived natural Flavone exerts anti-cancer action displaying HDAC inhibitory activities. *Int J Biochem Cell Biol* **39**: 1902–1914.

Chiappetta G, Ferraro A, Vuttariello E, Monaco M, Galdiero F, De Simone V *et al*. (2008). HMGA2 mRNA expression correlates with the malignant phenotype in human thyroid neoplasias. *Eur J Cancer* **44**: 1015–1021.

Dai Y, Chen S, Kramer LB, Funk VL, Dent P, Grant S. (2008). Interactions between bortezomib and romidepsin and belinostat in chronic lymphocytic leukemia cells. *Clin Cancer Res* **14**: 549–558.

Duong V, Bret C, Altucci L, Mai A, Duraffourd C, Loubersac J *et al* (2008). Specific activity of class II histone deacetylases in human breast cancer cells. *Mol Cancer Res* **6**: 1908–1919.

Duvic M, Vu J. (2007). Vorinostat in cutaneous T-cell lymphoma. *Drugs Today (Barc)* **43**: 585–599.

Earel Jr JK., VanOosten RL, Griffith TS. (2006). Histone deacetylase inhibitors modulate the sensitivity of tumor necrosis factor-related apoptosis-inducing ligand-resistant bladder tumor cells. *Cancer Res* **66**: 499–507.

Fagin JA, Matsuo K, Karmakar A, Chen DL, Tang SH, Koeffler HP. (1993). High prevalence of mutations of the p53 gene in poorly differentiated human thyroid carcinomas. *J Clin Invest* **91**: 179–184.

Fiore L, Pollina LE, Fontanini G, Casalone R, Berlingieri MT, Giannini R *et al* (1997). Cytokine production by a new undifferentiated human thyroid carcinoma cell line, FB-1. *J Clin Endocrinol Metab* **82**: 4094–4100.

Fusco A, Berlingieri MT, Di Fiore PP, Portella G, Grieco M, Vecchio G. (1987). One- and two-step transformations of rat thyroid epithelial cells by retroviral oncogenes. *Mol Cell Biol* **7**: 3365–3370.

Gallinari P, Di Marco S, Jones P, Pallaoro M, Steinkuhler C. (2007). HDACs, histone deacetylation and gene transcription: from molecular biology to cancer therapeutics. *Cell Res* **17**: 195–211.

Garcia-Manero G, Yang H, Bueso-Ramos C, Ferrajoli A, Cortes J, Wierda WG *et al* (2008). Phase 1 study of the histone deacetylase inhibitor vorinostat (suberoylanilide hydroxamic acid [SAHA]) in patients with advanced leukemias and myelodysplastic syndromes. *Blood* **111**: 1060–1066.

Glaser KB. (2007). HDAC inhibitors: clinical update and mechanism-based potential. *Biochem Pharmacol* **74**: 659–671.

Gore L, Rothenberg ML, O'Bryant CL, Schultz MK, Sandler AB, Coffin D *et al* (2008). A phase I and pharmacokinetic study of the oral histone deacetylase inhibitor, MS-275, in patients with

refractory solid tumors and lymphomas. *Clin Cancer Res* **14**: 4517–4525.

Hall MA, Cleveland JL. (2007). Clearing the TRAIL for Cancer Therapy. *Cancer Cell* **12**: 4–6.

Hess-Stumpp H, Bracker TU, Henderson D, Politz O. (2007). MS-275, a potent orally available inhibitor of histone deacetylases—the development of an anticancer agent. *Int J Biochem Cell Biol* **39**: 1388–1405.

Iervolino A, Iuliano R, Trapasso F, Viglietto G, Melillo RM, Carlomagno F *et al* (2006). The receptor-type protein tyrosine phosphatase J antagonizes the biochemical and biological effects of RET-derived oncoproteins. *Cancer Res* **66**: 6280–6287.

Inoue S, Mai A, Dyer MJ, Cohen GM. (2006). Inhibition of histone deacetylase class I but not class II is critical for the sensitization of leukemic cells to tumor necrosis factor-related apoptosis-inducing ligand-induced apoptosis. *Cancer Res* **66**: 6785–6792.

Insinga A, Monestiroli S, Ronzoni S, Gelmetti V, Marchesi F, Viale A *et al* (2005). Inhibitors of histone deacetylases induce tumor-selective apoptosis through activation of the death receptor pathway. *Nat Med* **11**: 71–76.

Jenuwein T, Allis CD. (2001). Translating the histone code. *Science* **293**: 1074–1080.

Johnstone RW, Frew AJ, Smyth MJ. (2008). The TRAIL apoptotic pathway in cancer onset, progression and therapy. *Nat Rev Cancer* **8**: 782–798.

Kelly WK, Marks PA. (2005). Drug insight: Histone deacetylase inhibitors—development of the new targeted anticancer agent suberoylanilide hydroxamic acid. *Nat Clin Pract Oncol* **2**: 150–157.

Kelly WK, O'Connor OA, Krug LM, Chiao JH, Heaney M, Curley T *et al* (2005). Phase I study of an oral histone deacetylase inhibitor, suberoylanilide hydroxamic acid, in patients with advanced cancer. *J Clin Oncol* **23**: 3923–3931.

Kummar S, Gutierrez M, Gardner ER, Donovan E, Hwang K, Chung EJ *et al* (2007). Phase I trial of MS-275, a histone deacetylase inhibitor, administered weekly in refractory solid tumors and lymphoid malignancies. *Clin Cancer Res* **13**: 5411–5417.

Lin Z, Bazzaro M, Wang MC, Chan KC, Peng S, Roden RB. (2009). Combination of proteasome and HDAC inhibitors for uterine cervical cancer treatment. *Clin Cancer Res* **15**: 570–577.

Macher-Goeppinger S, Aulmann S, Tagscherer KE, Wagener N, Haferkamp A, Penzel R *et al* (2009). Prognostic value of tumor necrosis factor-related apoptosis-inducing ligand (TRAIL) and TRAIL receptors in renal cell cancer. *Clin Cancer Res* **15**: 650–659.

Mahalingam D, Szegezdi E, Keane M, Jong S, Samali A. (2009). TRAIL receptor signalling and modulation: Are we on the right TRAIL? *Cancer Treat Rev* **35**: 280–288.

Mai A, Altucci L. (2009). Epi-drugs to fight cancer: from chemistry to cancer treatment, the road ahead. *Int J Biochem Cell Biol* **41**: 199–213.

Mai A, Massa S, Pezzi R, Simeoni S, Rotili D, Nebbioso A *et al* (2005). Class II (IIa)-selective histone deacetylase inhibitors. 1. Synthesis and biological evaluation of novel (aryloxopropenyl) pyrrolyl hydroxyamides. *J Med Chem* **48**: 3344–3353.

Mann BS, Johnson JR, Cohen MH, Justice R, Pazdur R. (2007). FDA approval summary: vorinostat for treatment of advanced primary cutaneous T-cell lymphoma. *Oncologist* **12**: 1247–1252.

Marks P, Rifkind RA, Richon VM, Breslow R, Miller T, Kelly WK. (2001). Histone deacetylases and cancer: causes and therapies. *Nat Rev Cancer* **1**: 194–202.

Marks PA. (2007). Discovery and development of SAHA as an anticancer agent. *Oncogene* **26**: 1351–1356.

Miller CP, Ban K, Dujka ME, McConkey DJ, Munsell M, Palladino M *et al* (2007). NPI-0052, a novel proteasome inhibitor, induces caspase-8 and ROS-dependent apoptosis alone and in combination with HDAC inhibitors in leukemia cells. *Blood* **110**: 267–277.

Miller CP, Rudra S, Keating MJ, Wierda WG, Palladino M, Chandra J. (2009). Caspase-8 dependent histone acetylation by a novel proteasome inhibitor, NPI-0052: a mechanism for synergy in leukemia cells. *Blood* **113**: 4289–4299.

Minucci S, Pelicci PG. (2006). Histone deacetylase inhibitors and the promise of epigenetic (and more) treatments for cancer. *Nat Rev Cancer* **6**: 38–51.

Mitsiades CS, Poulaki V, McMullan C, Negri J, Fanourakis G, Goudopoulou A *et al* (2005). Novel histone deacetylase inhibitors in the treatment of thyroid cancer. *Clin Cancer Res* **11**: 3958–3965.

Nappi TC, Salerno P, Zitzelsberger H, Carlomagno F, Salvatore G, Santoro M. (2009). Identification of Polo-like kinase 1 as a potential therapeutic target in anaplastic thyroid carcinoma. *Cancer Res* **69**: 1916–1923.

Nebbioso A, Clarke N, Voltz E, Germain E, Ambrosino C, Bontempo P *et al* (2005). Tumor-selective action of HDAC inhibitors involves TRAIL induction in acute myeloid leukemia cells. *Nat Med* **11**: 77–84.

Nikiforova MN, Kimura ET, Gandhi M, Biddinger PW, Knauf JA, Basolo F *et al* (2003). BRAF mutations in thyroid tumors are restricted to papillary carcinomas and anaplastic or poorly differentiated carcinomas arising from papillary carcinomas. *J Clin Endocrinol Metab* **88**: 5399–5404.

Pallante P, Berlingieri MT, Troncone G, Kruhoffer M, Orntoft TF, Viglietto G *et al* (2005). UbcH10 overexpression may represent a marker of anaplastic thyroid carcinomas. *Br J Cancer* **93**: 464–471.

Pallante P, Federico A, Berlingieri MT, Bianco M, Ferraro A, Forzati F *et al* (2008). Loss of the CBX7 gene expression correlates with a highly malignant phenotype in thyroid cancer. *Cancer Res* **68**: 6770–6778.

Portella G, Ferulano G, Santoro M, Grieco M, Fusco A, Vecchio G. (1989). The Kirsten murine sarcoma virus induces rat thyroid carcinomas *in vivo*. *Oncogene* **4**: 181–188.

Saltman B, Singh B, Hedvat CV, Wreesmann VB, Ghossein R. (2006). Patterns of expression of cell cycle/apoptosis genes along the spectrum of thyroid carcinoma progression. *Surgery* **140**: 899–905 discussion 905–6.

Scognamiglio A, Nebbioso A, Manzo F, Valente S, Mai A, Altucci L. (2008). HDAC-class II specific inhibition involves HDAC proteasome-dependent degradation mediated by RANBP2. *Biochim Biophys Acta* **1783**: 2030–2038.

Xu WS, Parmigiani RB, Marks PA. (2007). Histone deacetylase inhibitors: molecular mechanisms of action. *Oncogene* **26**: 5541–5552.

Yu C, Friday BB, Yang L, Atadja P, Wigle D, Sarkaria J *et al* (2008). Mitochondrial Bax translocation partially mediates synergistic cytotoxicity between histone deacetylase inhibitors and proteasome inhibitors in glioma cells. *Neuro Oncol* **10**: 309–319.

Supplementary Information accompanies the paper on the Oncogene website (http://www.nature.com/onc)